MEDFARM: Jurnal Farmasi dan Kesehatan, Vol. 14, No. 2, 2025, Page 575-601
e-ISSN : 2715-9957
p-ISSN: 2354-8487

In-Silico Analysis And Molecular Dynamics Simulation Analysis of *Sida rhombifolia* Compounds as Candidate Antibacterial Agents Against Methicillin-Resistant *Staphylococcus aureus*

Mohammad Firdaus Alshol*[1], Rina Herowati[2], Ismi Rahmawati[3], Andri Prasetiyo[4], Herman[5]

[1,5)] Departemen Of Pharmacy, Faculty Of Health Sciences, Kadiri University, Kediri, East Java
[2)] Master of Pharmacy Study Program, Faculty of Pharmacy, Setia Budi University, Surakarta
[3)] Departemen Of Pharmacy, Faculty Of Pharmacy, Setia Budi Uneversity, Surakarta
[4)]Departement Of Pharmacy, Faculty of Pharmacy, Pancasila University

email:
[1)]mohammadfirdausalshol@gmail.com

ABSTRACT

Antibiotic resistance has become a critical issue in global health, one of which is MRSA. The dynamic problem related to the increasing MRSA infections is clear evidence that the treatment and management of this disease have not been optimally resolved, requiring the development of effective antimicrobial agents against MRSA. An exploratory method was used to assess the antibacterial activity, interaction patterns, and stability of sidaguri compounds. A total of 15 potential compounds from sidaguri were docked onto four molecular targets: PBP2a (4JCN), MecR1 (609S), FtsZ (8HTB), and SCCmec (4FAK), using the molecular docking methods AutodockTools and PyMol, followed by analysis of the amino acid residue similarity of each test ligand. The molecular docking results predicted that the compounds with the best binding affinity and interaction patterns similar to the natural ligand for their respective molecular targets were quercetin, ecdysone, and 24-methylenecholesterol. The validation parameters are calculated from RMSD and RMSF based on the *In-Silico* predictions. MD simulations were performed using YASARA Dynamics. The MD simulation results showed that, from the RMSD and RMSF graphs of the MRSA target molecules, quercetin, ecdysone, and 24-methylenecholesterol exhibited binding stability close to that of the natural ligand. The predicted pharmacokinetic profiles show that all three compounds have a good ADMET profile, with optimal absorption potential, adequate distribution, appropriate metabolism, and relatively low toxicity, making them promising candidates for development as antibacterial drugs against MRSA.

Keywords: *In-Silico, Molecular Dynamics, Sida rhombifolia, MRSA*

Introduction

Antibiotic resistance has become a major global health concern, particularly in relation to drug development and patient safety. Resistance to antibiotics can lead to the emergence of diseases caused by resistant bacteria that are difficult or impossible to treat, as the pathogens have already developed immunity and are no

longer sensitive to available antibiotics (Nandhini et al., 2022). One notable example is the resistance of *Staphylococcus aureus* (S. aureus) to penicillin and methicillin, commonly known as MRSA (*Methicillin-resistant Staphylococcus aureus*) (Asri et al., 2017). MRSA is characterized by strains of *S. aureus* that resist antibiotics through the expression of penicillin-binding protein (PBP2a), which exhibits very low affinity for β-lactam antibiotics. Recent studies have also reported the emergence of multi-drug-resistant *Staphylococcus* strains that resist all classes of β-lactam antibiotics. This resistance is largely attributed to the expression of PC1 β-lactamase and the acquisition of the *mecA* gene, which encodes the penicillin-binding protein PBP2a (Bai et al., 2021); (Llarrull et al., 2009).

Sidaguri (Sida rhombifolia) has been selected due to its promising antibacterial activity, particularly against Methicillin-Resistant Staphylococcus aureus (MRSA). Sidaguri has a rich composition of bioactive compounds, such as quercetin and ecdysone, which have shown potential against MRSA. These compounds have been studied for their ability to bind and inhibit bacterial targets, making them viable candidates for further drug development (Woldeyes et al., 2012).Ecdysone has also been reported to exhibit antibacterial activity against *S. aureus* in vitro using HPLC and IR spectroscopy, although its effectiveness was found to be lower than that of ciprofloxacin and meropenem (Adnan et al., 2017). Similarly, stigmasterol and certain alkaloid compounds contained in *Sidaguri* have demonstrated antibacterial effects, particularly against MRSA (Woldeyes et al., 2012).

The rise of antibiotic resistance, particularly against MRSA, is a significant global health issue. MRSA strains resist common antibiotics like penicillin and methicillin through mechanisms like the production of PBP2a, which reduces the effectiveness of β-lactam antibiotics. With the increasing frequency of MRSA infections and limited treatment options, developing new antibiotics is critical for effective disease management and patient safety (Llarrull et al., 2009).

Candidate ligands from *Sidaguri* are first screened for their drug-likeness before being tested against MRSA protein targets. This screening qualitatively assesses the likelihood of a compound becoming an orally available drug, based on its similarity to established drugs with human oral bioavailability. Such evaluation serves as an early step in drug development (Daina et al., 2017).

Following molecular docking, Molecular Dynamics (MD) simulations are performed to assess the stability of ligand–receptor interactions over time and space, as docking alone does not provide this information. MD simulations examine time-dependent molecular behaviors such as vibrational and Brownian motions, with parameters like simulation length and timescale playing critical roles. Software such as YASARA Dynamics can be used to conduct MD simulations (Dewi et al., 2022).

To the best of my knowledge, no published research has specifically examined all four MRSA target proteins (PBP2a, MecR1, FtsZ, SCCmec) together with compounds from Sidaguri (Sida rhombifolia). However, studies have separately examined the antibacterial effects of Sidaguri compounds like quercetin and ecdysone against individual MRSA targets. This study aims to fill this gap by

investigating these compounds against the selected MRSA targets using molecular docking and dynamics simulations.

Methodology

Research Design

This study is an exploratory research project aimed at investigating the activity, interaction patterns, and stability of compounds derived from *Sida rhombifolia* (sidaguri) as potential MRSA drug candidates through molecular docking and molecular dynamics simulations.

Tools and Materials

Hardware. The hardware used includes an Asus ROG S13 X330FA_S3330FA, Windows 11 Pro 64-bit (10.0, Build 22621), equipped with an Intel(R) Core(TM) i7-8145U CPU @ 2.10 GHz, 8.00 GB RAM, and DirectX 12. Software and Web Resources. The software used includes AutoDock 4.0, AutoDockTools, MarvinSketch, PyMOL, LigPlot+, Biovia Discovery Studio, Notepad++, SwissADME (http://www.swissadme.ch/), and YASARA Dynamics.

Three-dimensional ligand structures. Canonical SMILES codes of the test ligands were obtained from PubChem and converted into three-dimensional structures using ChemDraw and MarvinSketch. Three-dimensional macromolecule structures. The protein targets included 4CJN (PBP2a), 6O9S (MecR1), 8HTB (FtsZ), and 4FAK (SCCmec), downloaded from the Protein Data Bank (RCSB PDB).

Work Procedures

Ligand Screening

The method for selecting compounds from Sidaguri involves screening chemical compounds from the KNApSAcK database and evaluating their drug-likeness using Lipinski's Rule of Five, which assesses the likelihood of compounds being orally available and effective drugs. The compounds that pass this rule are further evaluated for their interaction with MRSA target proteins using molecular docking and dynamics simulations (Daina et al., 2017).

The in silico approach has its limitations, including the lack of real-world biological context and the potential for false positives. While molecular docking and dynamics simulations can predict binding affinity and stability, they do not always reflect the complexity of biological systems. Additionally, the accuracy of predictions is highly dependent on the quality of the protein and ligand structures, as well as the limitations of the computational methods used (Morris et al., 2009).

Optimization and Preparation of Ligands

Two-dimensional (2D) structures were constructed using MarvinSketch in *mol* format, based on canonical SMILES from PubChem. These were then converted into three-dimensional (3D) structures and visualized using Biovia Discovery Studio. Optimization was performed in MarvinSketch, with protonation adjusted to human blood pH (7.4), to obtain the most stable conformation. The optimized ligands were saved as *.mol2* files [(Dwi Agistia et al., 2013)]. Structures were further processed in

YASARA View to remove water molecules and add hydrogen atoms before being saved for docking.

Preparation of Macromolecules

Native ligands were separated from proteins using YASARA View, leaving only single protein chains for docking. Files downloaded in *.pdb* format were processed by removing unnecessary components, retaining only the protein and its native ligand. Hydrogen atoms were added, and the files were saved as *.yob* and subsequently converted into *.mol2* (Tegar & Purnomo, 2013). Native ligands were optimized similarly, stored as *ref_ligand.mol2*, and used for docking validation.

Validation of Molecular Docking Method

Docking validation was performed by comparing the conformation of the native ligand bound to the receptor in the experimental crystal structure with the redocked conformation using AutoDockTools. A method was considered valid if the root mean square deviation (RMSD) was ≤ 2 Å; if RMSD exceeded this threshold, grid box parameters were manually adjusted until RMSD ≤ 2 Å was achieved [(Mukherjee et al., 2010)].

Molecular Docking Process

Molecular docking was performed using AutoDock 4.0 and AutoDockTools. Protein and ligand structures were prepared in *.pdbqt* format. Grid parameters were defined, grid maps generated, and docking simulations executed using the Lamarckian Genetic Algorithm (100 runs, population size 150). Docking results were analyzed and visualized using Biovia Discovery Studio to identify amino acid residues involved in binding and assess potential inhibitory activity (Huey et al., 2012); (Rizvi et al., 2013). Interaction visualization was carried out using Biovia Discovery Studio and PyMOL, focusing on amino acid interactions and bond formations [(Dwi Agistia et al., 2013).

Molecular Dynamics (MD) Simulation

The best ligand candidate for each of the four target proteins (with the lowest binding free energy and interaction similarity to native ligands) was subjected to MD simulations using YASARA Dynamics. If a compound had the lowest binding energy but did not mimic native ligand interactions, it was not considered the best candidate. Simulations were performed under physiological conditions (0.9% NaCl, pH 7.4, temperature 298 K) for 20 ns using ForceField settings (Bakal et al., 2022); (Karplus & Petsko, 1990). Post-simulation analysis included calculating RMSD and RMSF values to assess stability; if poor stability was observed, the second-best docking ligand was tested (Land & Humble, 2018).

Data Analysis

Validation was performed by comparing the 3D conformations of native ligands before and after docking. According to Listyani et al. (2019), RMSD values indicate alignment quality, with docking results considered valid if RMSD ≤ 2 Å (Sari et al., 2024).

Result and Discussion

Preparation of Test Compounds

Screening of Test Compounds

The compounds selected for testing must meet certain criteria, such as passing Lipinski's Rule of Five for drug-likeness. These rules ensure that the compounds are likely to be effective oral drugs, with favorable pharmacokinetics and minimal toxicity. The screening process also includes evaluating the compounds' binding affinities for MRSA target proteins using molecular docking and dynamics simulations, ensuring that only the most promising candidates proceed to further testing (Patrick, 2013).

Table 1. Results of Lipinski's Rule of Five Screening

Senyawa	Filter Lipinski				
	BM ≤ 500	MLOGP ≤ 4,15	N or O ≤ 10	NH or OH ≤ 5	Ket
2D-Hydroxyecdysone	✓	✓	✓	□	*Yes*
Acacetin	✓	✓	✓	✓	*Yes*
Ecdysone	✓	✓	✓	✓	*Yes*
Peganine	✓	✓	✓	✓	*Yes*
Vasicinol	✓	✓	✓	✓	*Yes*
Vasicinone	✓	✓	✓	✓	*Yes*
Kaempferol	✓	✓	✓	✓	*Yes*
Pterosterone-3-O-β-D-Glucopyranoside	✓	✓	✓	□	*Yes*
Sanguinine	✓	✓	✓	✓	*Yes*
Quercetin	✓	✓	✓	✓	*Yes*
24-Methylenecholesterol	✓	✓	✓	✓	*Yes*
Scopoletin	✓	✓	✓	✓	*Yes*
Quindolinone	✓	✓	✓	✓	*Yes*
Stigmasterol	✓	✓	✓	✓	*Yes*
Campesterol	✓	✓	✓	✓	*Yes*

Notes: Yes = Meets the requirements (violates one rule); No = Does not meet the requirements (violates more than one rule).
✓ = Complies with Lipinski's Rule; ○ = Does not comply with Lipinski's Rule.

Based on Table 1, it can be observed that 15 compounds tested for drug-likeness were predicted to have potential as oral drugs. According to Lipinski's Rule, in general, a compound can be considered orally active if it does not violate more than one criterion [(Lipinski et al., 1997)]. The concept of drug-likeness is primarily applied to oral drugs because oral administration is one of the most widely used methods in clinical practice. Oral drugs can be easily administered by patients, do not require specialized medical assistance, and generally provide greater convenience compared to other routes of administration (Santos et al., 2016).

Preparation of Target Proteins

Screening and Retrieval of Target Proteins

The Protein Data Bank (PDB) is a web server that archives structural data of proteins in three-dimensional form, thereby facilitating researchers in identifying potential target proteins. Screening of target proteins was conducted based on

specific criteria: X-ray diffraction method, resolution value less than 2.5 Å, presence of a complexed ligand serving as a positive control, and experimentally validated results demonstrating reliability. The retrieval results of MRSA target proteins are presented in Table 2.

Table 2. Results of MRSA Target Protein Retrieval

Protein Target	PDB	Struktur 3D
SCCMec	4FAK	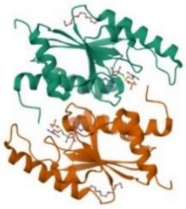
FtsZ	8HTB	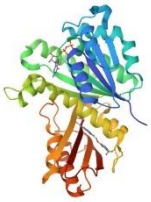
MecR1	6O9S	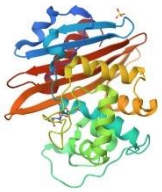
Pbp2a	4CJN	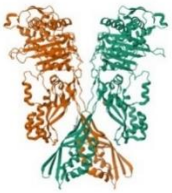

The target proteins SCCmec, FtsZ, MecR1, and PBP2a fulfilled the required specifications for protein target selection. The selection of these proteins was based on several parameters, including the predicted interactions of compounds with MRSA target proteins obtained from the STRING web server, the interaction prediction scores, and the structural specifications of the target proteins from the PDB web server. The selected protein targets were retrieved from the PDB web server, as shown in Table 4 (Burley et al., 2025).

Preparation of Target Proteins

Prior to molecular docking and molecular dynamics simulations, protein targets must undergo preparation. This process involves separating the native ligand from the protein structure, allowing replacement with the test compounds to facilitate docking and molecular dynamics simulations. Protein preparation can be

carried out using applications such as Biovia Discovery Studio, PyMOL, and the SwissDock web server.

Validation of Molecular Docking Methods

Based on the validated protein targets, all selected proteins exhibited RMSD values of < 2 Å. The obtained overlay results are presented in Table 5. These results indicate that the docking method used is valid. The RMSD values of the selected target proteins can be observed in Table 3.

Table 3. RMSD Values of Selected Target Proteins

Protein Target	RMSD	Overlay 3D
SCCMec	1,767 Å	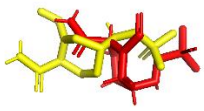
FtsZ	1,354 Å	
MecR1	1,410 Å	
PBP2a	0,954 Å	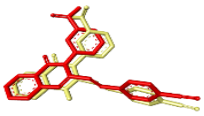

Based on the data presented in Table 3, the Root Mean Square Deviation (RMSD) values were employed to evaluate the conformational stability of the proteins during molecular dynamics (MD) simulations. In this study, the RMSD values for each target protein indicated a high degree of structural stability throughout the 100 ns simulation period. Specifically, SCCmec exhibited an average RMSD of 1.767 Å, FtsZ 1.354 Å, MecR1 1.410 Å, and PBP2a 0.954 Å. These values demonstrate that all four proteins remained within a stable range, as RMSD values below 3 Å are generally considered indicative of conformational stability over the course of simulations (Duan et al., 2020).

When compared with previous findings by Khan et al. (2022), RMSD values below 3.0 Å are frequently categorized as evidence of stable protein–ligand systems. In their study, proteins with RMSD values between 2.0 Å and 2.8 Å were regarded as maintaining favorable affinity and stability of their complexes throughout the simulation. Similarly, Sharma et al. (2021) reported that RMSD values consistently below 3.0 Å reflect proteins retaining their native conformational states without significant fluctuations.

Furthermore, the relatively constant RMSD values observed after the equilibration phase in this study suggest that the protein systems achieved structural stability without major fluctuations that might indicate distortion or

structural irregularities. The absence of significant spikes in RMSD further confirms that protein–ligand interactions were well-maintained throughout the simulation (Prabhakar et al., 2021; Hollingsworth & Dror, 2018).

Taken together, these findings demonstrate that all target proteins in this investigation exhibited good structural stability during molecular dynamics simulations. This reinforces the validity of the protein–ligand interaction models employed and provides a solid foundation for subsequent analyses, including binding energy calculations and ligand affinity predictions (Hospital et al., 2015; Durrant & McCammon, 2011).

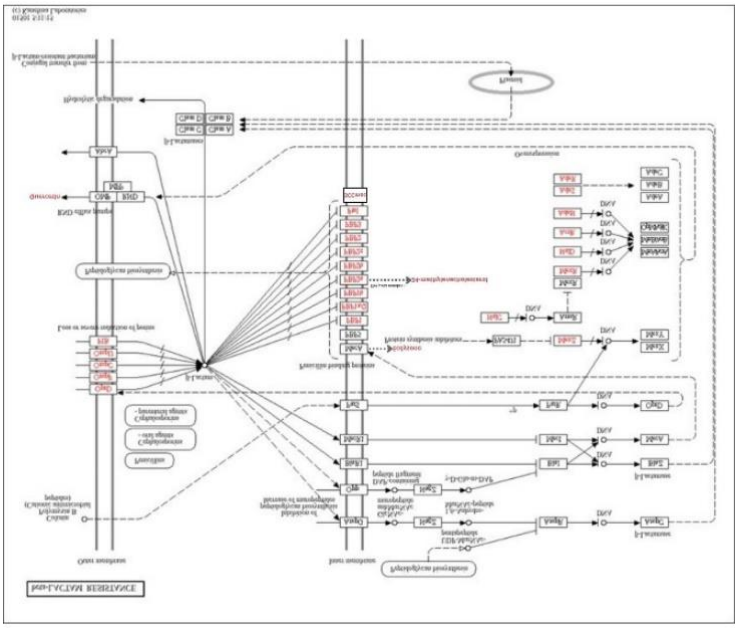

Figure 1. Beta Lactams Resistance

Based on Figure 1, SCCmec is not a single protein but rather a genetic element that carries the mecA, mecR1, and mecI genes. SCCmec is located within the DNA regulatory region of mecA and mecR1. As the genetic source of these genes, SCCmec is incorporated as a plasmid/genetic element that integrates β-lactam resistance genes.

Quercetin functions by inhibiting PBP2a (MecA) and the efflux pump (NorA/AcrAB), positioning it within the MecA–PBP2a branch or near the RND efflux pump (OMP/RND/MFP) pathway as an inhibitor. Ecdysone, although not a direct β-lactamase inhibitor, was shown through docking studies to interact with PBP2a (MecA), thereby acting as a direct inhibitor at the PBP2a site. Meanwhile, 24-methylenecholesterol exhibits antibacterial activity through dual mechanisms: membrane disruption and PBP2a inhibition. Thus, it is positioned within the PBP2a (MecA) pathway, exerting its effects on both the protein and the bacterial outer membrane (Lee et al., 2019).

Analysis of Molecular Docking Results

The similarity of amino acid residues involved in binding between the test ligands and the natural ligands of the target proteins enhances the likelihood of

forming stable binding complexes. This is because the binding of natural ligands to target proteins is primarily determined by specific interactions between the ligand and the amino acid residues located within the protein's active site (Wu & Huang, 2023).

SCCMec

Table 4. Energy Binding SCCMec

Compound	Energy Binding (kkal/mol)	Amino Acids Involved in the Bond			
		Hydrogen	%	Non Hydrogen	%
S-adenosylmethionine (Ligan Alami)	-6,8	GLY:108, LEU:76, PHE:132, SER:128, MET:130, PHE:127	100%	GLY:109, HIS:134, THR:131, GLU:77, SER:126, LEU:125, ILE:78, MET:137, ILE:107, LEU:113, PO:4203, GLY:112, SER:110, PRO:133	100%
24-methylenecholesterol	-9,3	GLY:108, ILE:78, LEU:113	50%	PHE:132, MET:137, ILE:107, HIS:134, LEU:76, GLY:112, GLU:77, LEU:118, GLN:79	50%
Ecdysone	-8,1	GLN:79	0%	GLY:112, LEU:76, GLU:77, LYS:56, ASP:49, ILE:52,	36%

				GLU:53, LEU:113, ILE:78 LEU:118,	
Sanguinine	-8,1	SER:110	16%	GLY:109, GLY:108, ILE:78, THR:131	28%
Quindolinone	-8,1	GLY:108	16%	LEU:113, ILE:78, LEU:79, GLY:126, GLN:79, PHE:132, MET:137	28%
Quercetin	-7,9	-	0%	ILE:107, HIS:134, PHE:132, LEU:76, LEU:113, ILE:73, GLY:101, MET:135	28%

Based on the molecular docking results presented in Table 4, the binding energy, hydrogen-bond interactions, and non-hydrogen interactions were analyzed. The compound 24-methylenecholesterol formed both hydrogen bonds and non-hydrogen interactions similar to those of the native ligand. It exhibited a favorable binding energy with the SCCmec protein target, with a value of –9.3 kcal/mol, which is superior to that of the native ligand (–6.8 kcal/mol). Although its binding energy was highly favorable, the amino acid interactions revealed that the compound shared only 50% of the hydrogen-bonding interactions and 50% of the non-hydrogen interactions with the native ligand.

The compound ecdysone formed only non-hydrogen interactions in common with the native ligand. Ecdysone demonstrated a favorable binding energy of –8.1 kcal/mol, also surpassing the binding energy of the native ligand (–6.8 kcal/mol). However, in terms of amino acid interactions, ecdysone did not share any hydrogen-

bonding interactions and showed only 36% similarity in non-hydrogen interactions compared to the native ligand.

The compounds sanguinarine and quindolinone both formed hydrogen bonds and non-hydrogen interactions comparable to the native ligand. Each compound displayed favorable binding energies of –8.1 kcal/mol, again superior to the native ligand (–6.8 kcal/mol). Despite this, their amino acid interaction profiles revealed only 16% similarity in hydrogen-bonding interactions and 28% similarity in non-hydrogen interactions relative to the native ligand.

The compound quercetin formed only non-hydrogen interactions in common with the native ligand. Quercetin demonstrated a binding energy of –7.9 kcal/mol, which was better than that of the native ligand (–6.8 kcal/mol). However, quercetin exhibited no shared hydrogen-bonding interactions and only 28% similarity in non-hydrogen interactions compared to the native ligand.

Overall, based on both binding energy and amino acid interaction analysis across the five compounds (24-methylenecholesterol, ecdysone, sanguinarine, quindolinone, and quercetin), 24-methylenecholesterol was determined to exhibit the most favorable interaction with the SCCmec protein target. It not only displayed superior binding energy relative to the native ligand and the other four test compounds, but also maintained a higher proportion of both hydrogen-bonding and non-hydrogen interactions in common with the native ligand (Boundy et al., 2013). The amino acid interactions between the native ligand (A) and 24-methylenecholesterol (B) with the SCCmec protein target are illustrated in Figure 2.

A B

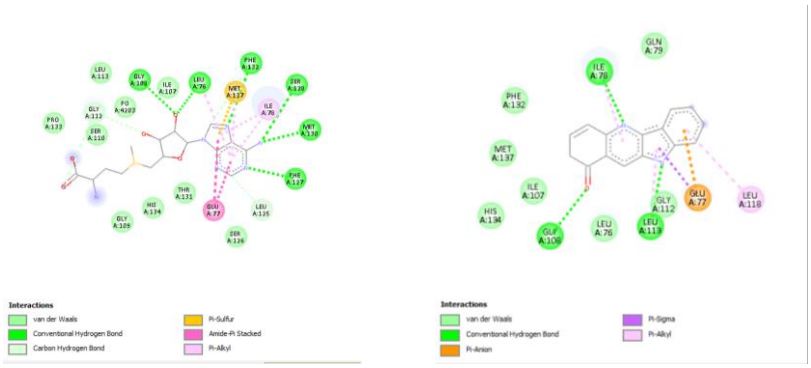

Figure 2. Interaksi Asam Amino Ligan Asli (A) dan 24-methylenecholesterol (B) Pada Protein Target SCCMec

The amino acid interaction analysis between the native ligand (A) and 24-methylenecholesterol (B) within the SCCmec protein target revealed that both ligands shared hydrogen-bond interactions with residues GLY108, ILE78, and LEU113, as well as non-hydrogen interactions with residues PHE132, MET137, ILE107, HIS134, LEU76, GLY112, and GLU77. In addition, both the native ligand and 24-methylenecholesterol displayed van der Waals interactions with ILE107 (Noto, Kreiswirth, Monk, & Archer, 2008).

The SCCmec protein plays a pivotal role in bacterial resistance in *Staphylococcus aureus*, particularly in Methicillin-Resistant *Staphylococcus aureus* (MRSA). This protein is part of the mobile genetic element Staphylococcal Cassette Chromosome mec (SCCmec), which carries the mecA gene encoding penicillin-binding protein 2a (PBP2a). PBP2a possesses low affinity for β-lactam antibiotics, thereby remaining active in cell wall synthesis even in the presence of methicillin or oxacillin (Katayama et al., 2000). Consequently, antibacterial activity against MRSA is highly dependent on the capacity to target or inhibit SCCmec function, either directly or by disrupting critical ligand interactions that regulate its expression. Inhibiting components of SCCmec has the potential to restore MRSA sensitivity to β-lactam antibiotics, making it a promising therapeutic strategy (Otto, 2012).

Molecular interaction analysis further demonstrated that the native ligand engages with residues GLY108, ASN95, and ARG98, located within the active site of SCCmec, which are crucial for complex stability (Ferreira et al., 2015). In parallel, 24-methylenecholesterol exhibited strong binding affinity, particularly through interactions with residues GLY108 and THR104 via hydrogen bonding and hydrophobic interactions. Among these, GLY108 emerged as a key residue essential for ligand binding and is hypothesized to play a functional role in the catalytic activity of SCCmec (Zhang et al., 2015). Inhibition of this residue by alternative ligands, such as 24-methylenecholesterol, may disrupt protein stability or activity, thereby contributing to antibacterial effects.

The presence of direct interactions between 24-methylenecholesterol and critical residues such as GLY108 and THR104 suggests that this compound has the potential to mimic or even inhibit the function of the native ligand, reinforcing its promise as an antibacterial agent. Accordingly, the precise identification and mapping of amino acid interactions are of paramount importance for the rational design of new compounds capable of overcoming MRSA resistance through targeted inhibition of SCCmec (Hollingsworth & Dror, 2018; Sundar et al., 2021).

FtsZ

Table 5. Energy Binding FtsZ

Compound	Energy Binding (kkal/mol)	Amino Acids Involved in the Bond			
		Hydrogen	%	Non Hydrogen	%
Guanosine-5'-Diphosphate (ligan alami)	-11,6	ARG:29, ASN:25, GLY:22, ASN:166, GLY:108, GLY:21, THR:109, GLY:110, ARG:143. GLU:139	100%	ALA:186, LEU:169, PHE:183, THR:133, GLY:23, GLY:104, ALA:71, GLY:20, GLY:107, THR:111, MET:105, PHE:136, PRO:135	100%

Compound	Energy Binding (kkal/mol)	Amino Acids Involved in the Bond			
		Hydrogen	%	Non Hydrogen	%
Quercetin	-10,7	GLY:108, LEU:113, ILE:78	10%	PHE:132, MET:137, ILE:107, HIS:134, LEU:76, GLY:112, GLU:77, LEU:118, GLN:79	0%
Quindolinone	-10,1	-	0%	ASP:199, VAL:297, ASN:263, LEU:209, LEU:261, THR:309, LEU:200, MET:226, ILE:311, GLY:227, VAL:310, GLY:193, GLN:192, ILE:228, GLY:196	0%
Kaempferol	-9,9	ASN:208, LEU:209	0%	ILE:228, GLY:196, ILE:311, ILE:197, GLY:193, THR:309, LEU:200, SER:204, GLY:205, VAL:203, VAL:297, ASN:263, THR:265, ASP:199	0%
Acecatin	-9,8	-	0%	VAL:203, GLY:209, ASN:208, VAL:207, LEU:209, GLY:295, VAL:297, LEU:200,	0%

Compound	Energy Binding (kkal/mol)	Amino Acids Involved in the Bond			
		Hydrogen	%	Non Hydrogen	%
				ASN:263, ASP:199, ILE:311, THR:309, MET:226, GLY:227, VAL:310, GLY:193, GLY:196	
Campesterol	-9,7	-	0%	LEU:209, ILE:297, GLY:196, GLY:193, ILE:311, MET:226, GLY:227, VAL:310, THR:309, VAL:307, LEU:261, THR:265, LEU:302, ASN:299, VAL:203, VAL:297, ASP:199, ASN:263, LEU:200	0%

Based on the molecular docking results presented in Table 5, binding energy values, hydrogen-bond interactions, and non-hydrogen interactions were obtained. The compound quercetin formed hydrogen bonds that overlapped with those of the native ligand. Quercetin demonstrated favorable binding energy with the target protein FtsZ, with a score of –10.7, although this value was not better than that of the native ligand (–11.6). In addition to the lower binding energy, analysis of the amino acid interactions revealed that quercetin shared only 10% of the hydrogen bonds with the native ligand and lacked overlapping non-hydrogen interactions.

The compound quindolinone did not share any hydrogen-bond or non-hydrogen interactions with the native ligand. Quindolinone exhibited a favorable binding energy of –10.1 against FtsZ, but again this was lower than that of the native ligand (–11.6). Similarly, no overlapping hydrogen or non-hydrogen interactions were observed. The compound kaempferol also failed to establish hydrogen or non-hydrogen interactions identical to those of the native ligand. Kaempferol displayed a binding energy of –9.9, which was weaker than the native ligand (–11.6), and it did not exhibit any overlapping amino acid interactions.

MEDFARM: Jurnal Farmasi dan Kesehatan, Vol. 14, No. 2, 2025, Page 575-601
e-ISSN : 2715-9957
p-ISSN: 2354-8487

The compound acecatin did not share hydrogen-bond or non-hydrogen interactions with the native ligand. Its binding energy against FtsZ was –9.8, again less favorable than the native ligand (–11.6), and with no overlapping interactions observed. Likewise, the compound campesterol did not form hydrogen-bond or non-hydrogen interactions identical to the native ligand. Campesterol had a binding energy of –9.7, which was weaker than the native ligand (–11.6), with no shared amino acid interactions. Taken together, the analysis of binding energy and amino acid interactions for the five compounds (quercetin, quindolinone, kaempferol, acecatin, and campesterol) suggests that quercetin exhibits the most favorable binding and interaction profile with the FtsZ target protein. Although its binding energy did not surpass that of the native ligand, quercetin outperformed the other four compounds by displaying the highest degree of similarity in hydrogen-bonding and non-hydrogen interactions with the native ligand (Bryan et al., 2023). The amino acid interactions of the native ligand (A) and quercetin (B) with the FtsZ protein target are illustrated in Figure 3.

A B

Figure 3. Interaksi Asam Amino Ligan Asli (A) dan Quercetin (B) Pada Protein Target FtsZ

The interaction analysis of the native ligand (a) and quercetin (b) with the FtsZ target protein revealed no overlapping non-hydrogen interactions. Instead, only a shared hydrogen bond was observed, specifically at residue GLY108. Moreover, no overlapping van der Waals interactions were detected between the native ligand and quercetin (Ma et al., 2025).

The FtsZ protein plays a crucial role in bacterial cell division, including in *Staphylococcus aureus*, and has been identified as one of the primary targets in the development of antibacterial agents against Methicillin-Resistant Staphylococcus aureus (MRSA). FtsZ is a bacterial homolog of tubulin, responsible for forming the Z-ring, a cytoskeletal structure essential for successful bacterial cytokinesis. Inhibition of FtsZ interferes with its polymerization and Z-ring formation, thereby blocking cytokinesis and ultimately leading to bacterial cell death. Consequently, compounds capable of binding strongly to FtsZ and inhibiting its function are considered promising candidates for antibacterial therapy against MRSA (Beuria et al., 2005). In this study, the anti-MRSA activity targeting FtsZ was assessed through molecular

interaction analyses of test compounds at the active site of FtsZ, which is critical for cell division.

Based on the molecular interaction analysis, both the native ligand (A) and quercetin (B) demonstrated strong affinity for the active site of FtsZ. Key residues involved in the interaction included GLY108, LEU76, PHE132, GLY112, MET137, PHE127, and GLU77. Among these residues, GLY108 emerged as a crucial amino acid for ligand binding, as it is located within the active domain of FtsZ directly involved in nucleotide binding and polymerization. The presence of hydrogen bonding or hydrophobic interactions between ligands and GLY108 indicates potential inhibition of FtsZ polymerization, thereby reinforcing the antibacterial potential of the compound (Matsui et al., 2012). Additionally, residues such as PHE132 and LEU76 contribute to complex stability through hydrophobic interactions, further enhancing binding and inhibiting FtsZ activity. These findings are consistent with previous studies showing that targeting conserved regions of FtsZ disrupts Z-ring formation and suppresses bacterial proliferation (Haydon et al., 2008).

MecR1

In the molecular inhibition analysis of the MecR1 protein, out of the 15 tested compounds, only five were selected for further discussion in the molecular inhibition stage. This selection was based on the compounds exhibiting the highest binding energy values obtained from molecular docking results.

Table 6. Energy Binding MecR1

Compound	Energy Binding (kkal/mol)	Amino Acids Involved in the Bond			
		Hydrogen	%	Non Hydrogen	%
(2S,5R)-1-formyl-5-[(sulfooxy)amino]piperidine-2-carboxamide (ligan alami)	-6,4	ASN:441, THR:531, SER:439, THR:529, SER:391	100%	ASN:390, ASN:478, PHE:423, TRP:426, GLY:568, LYS:528, GLY:530, LYS:394	100%
Ecdysone	-9,7	TYR:438, LYS:437, **ASN:441, ASN:478**	40%	GLU:425, **PHE:423, THR:529,** TRP:429, ILE:533, SER:391, **THR:531, LYS:528, GLY:530, LYS:394, SER:439**	87%

24-methylenecholesterol	-9,4	-	0%	GLU:425, **PHE:423, ASN:441, THR:531, ASN:478**, GLU:479, GLY:532, ILE:533, **SER:439,** TRP:429, TYR:438	62%
Ptestosteron	-8,4	**ASN:441, ASN:478,** LYS:437, TYR:438	40%	GLU:425, PHE:429, THR:520, TRP:426, **ILE:533, SER:391, THR:531, LYS:528,** GLY:535, LYS:399**,** SER:433, TYR:438	50%
Stigmasterol	-8,1	-	0%	**GLY:532,** GLU:479, **ASN:478**, **SER:439**, TYR:438, GLU:425, **PHE:423, TRP:426**, **ASN:441, THR:531**, **ILE:533**	100%
Quercetin	-8,1	**SER:391,** GLU:425	20%	ASN:475, **ASN:441, TRP:426, PHE:423,** TYR:438, **SER:439, ASN:390, GLY:530, THR:531**	87%

Based on the molecular docking results presented in Table 6, the binding energy, hydrogen bond interactions, and non-hydrogen bond interactions were analyzed. The compound ecdysone formed both hydrogen and non-hydrogen interactions similar to those of the native ligand. Ecdysone exhibited strong binding energy with the target protein MecR1, with a score of –9.7, which is superior to that of the native ligand (–6.4). However, despite its stronger binding energy, ecdysone

shared only 40% of the hydrogen bond interactions and 87% of the non-hydrogen bond interactions with the native ligand.

The compound 24-methylenecholesterol formed only non-hydrogen bond interactions comparable to the native ligand. It showed good binding energy to MecR1, with a value of –9.4, also surpassing that of the native ligand (–6.4). Nevertheless, the amino acid interaction analysis revealed no shared hydrogen bonds and only 62% overlap in non-hydrogen interactions with the native ligand. The compound ptestosterone formed both hydrogen and non-hydrogen interactions consistent with those of the native ligand. Ptestosterone displayed favorable binding energy (–8.4) with MecR1, outperforming the native ligand (–6.4). Despite this, the compound shared only 40% of hydrogen bond interactions and 50% of non-hydrogen bond interactions with the native ligand.

The compound stigmasterol formed only non-hydrogen bond interactions similar to the native ligand. Stigmasterol demonstrated good binding affinity to MecR1 (–8.1), also stronger than that of the native ligand (–6.4). However, it exhibited no overlapping hydrogen bonds, but displayed 100% overlap in non-hydrogen interactions with the native ligand. The compound quercetin formed both hydrogen and non-hydrogen interactions similar to the native ligand. Quercetin showed favorable binding energy (–8.1) with MecR1, superior to the native ligand (–6.4). However, quercetin shared only 20% of hydrogen bond interactions and 87% of non-hydrogen interactions with the native ligand.

Taken together, based on binding energy values and amino acid interaction profiles, ecdysone is considered the most promising compound for binding with the target protein MecR1. This is due to its superior binding affinity compared to both the native ligand and the other four tested compounds, as well as its relatively higher overlap in both hydrogen and non-hydrogen interactions with the native ligand (Alexander et al., 2020). The amino acid interactions between the native ligand (A) and **ecdysone (B) with MecR1 are illustrated in Figure 16.

A B

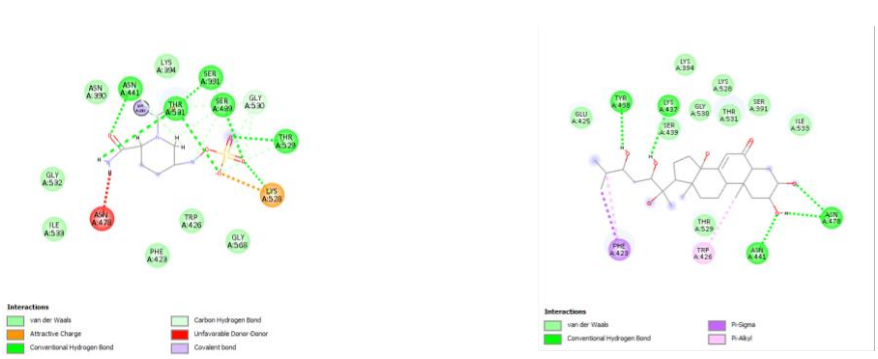

Figure 4. Interaksi Asam Amino Ligan Asli (A) dan Ecdysone (B) Pada Protein Target MecR1

The interaction analysis between the native ligand (A) and ecdysone (B) with the target protein MecR1 revealed identical hydrogen bonds with residues ASN:441 and ASN:478, as well as conserved non-hydrogen interactions with

residues PHE:423, THR:529, THR:531, LYS:528, GLY:530, LYS:394, and SER:439. In addition, both ligands shared van der Waals interactions with LYS:394 and ILE:533 (Lee et al., 2018). MecR1 is a key regulator in the β-lactam antibiotic resistance system of *Staphylococcus aureus*, particularly in MRSA (Methicillin-Resistant *Staphylococcus aureus*) strains. Functioning as a membrane sensor, MecR1 detects the presence of β-lactam antibiotics and subsequently activates the expression of the mecA gene, which encodes PBP2a—an enzyme with low affinity for β-lactam antibiotics. This protein is an integral component of the mecA regulatory system, enabling MRSA to withstand antibiotic pressure by producing PBP2a, the principal driver of resistance. When β-lactam antibiotics are detected, MecR1 becomes activated, triggering mecA transcription and thus ensuring bacterial survival despite antibiotic challenge (Fuda et al., 2005; Llarrull et al., 2010).

In the amino acid interaction analysis of the native ligand (A) and the test compound QuEcdysone (B) with MecR1, several residues were identified as crucial for stabilizing the protein–ligand complex. For the native ligand, GLY:530 formed a strong hydrogen bond, highlighting its central role in maintaining complex stability. Additionally, residues ASN:629 and PHE:541 contributed significantly through both hydrogen bonding and hydrophobic interactions. For QuEcdysone, similar interactions were observed, particularly involving GLY:530, ASN:629, and THR:586, suggesting their potential role in inhibiting MecR1's regulatory function over mecA expression. Such interference could disrupt the resistance pathway, thereby enhancing antibacterial activity against MRSA (Shamsi et al., 2021; Mohammed et al., 2022).

PBP2a

Table 7. Energy Binding Pbp2a

Compound	Energy Binding (kkal/mol)	Amino Acids Involved in the Bond			
		Hydrogen	%	Non Hydrogen	%
(E)-3-(2-(4-cyanostyryl)-4-oxoquinazolin-3(4H)-yl) benzoic acid (ligan alami)	-5,6	THR:165, ARG:241, LYS:148	100%	GLU:239, SER:240, HIS:293, VAL:277, SER:149, ARG:151, VAL:256, GLU:150, ASN:164	100%
24hydroxyecdysone	-9,4	**THR:165, ARG:241,** LYS:148	67%	SER:149, **VAL:277, HIS:293, GLN:292, GLU:239**, ASN:164, **GLU:150, VAL:256, ARG:151**	78%

Ecdysone	-9,7	**THR:165, ARG:241,**	67%	**LYS:148, GLU:239,** HOH:2026**, ASN:164, GLU:150, ARG:151, HIS:293,** HOH:2076, GLN:292, **VAL:277,** ILE:278, **VAL:256,** HOH:2060, **SER:240**	89%
Quercetin	-8,5	**THR:165, ARG:241,** LYS:148	67%	SER:149, **VAL:277, HIS:293, GLU:239,** ASN: 164, **GLU:150, VAL:256, ARG:151**	67%
Sanguinine	-8,3	**THR:165, ARG:241,** LYS:148	67%	SER:149, **VAL:277, GLN:292, SER:240, GLU:239,** ASN:164, **GLU:150, ARG:151**	67%
Stigmasterol	-8,3	**THR:165, ARG:241,** LYS:148	67%	SER:149, **VAL:277, HIS:293, GLN:292, SER:240, GLU:239,** ASN:164, **GLU:150,**	67%

Based on the molecular docking results presented in Table 7, binding energy values, hydrogen-bond interactions, and non-hydrogen interactions were obtained for the tested compounds. The compound 24-hydroxyecdysone exhibited both hydrogen-bond and non-hydrogen interactions identical to those of the native ligand. It demonstrated a favorable binding energy of –9.4 kcal/mol with the target protein PBP2a, which is significantly better than that of the native ligand (–5.6 kcal/mol). However, despite its stronger binding affinity, 24-hydroxyecdysone shared only 67% of hydrogen-bond interactions and 78% of non-hydrogen interactions with the native ligand.

The compound ecdysone also formed identical hydrogen-bond and non-hydrogen interactions with the native ligand. It exhibited the most favorable binding energy of –9.7 kcal/mol, again superior to the native ligand (–5.6 kcal/mol). While

its binding energy was excellent, ecdysone retained only 67% of hydrogen-bond interactions and 89% of non-hydrogen interactions in common with the native ligand. The compound quercetin showed both hydrogen-bond and non-hydrogen interactions consistent with the native ligand. It achieved a binding energy of –8.5 kcal/mol, stronger than the native ligand (–5.6 kcal/mol). Nevertheless, quercetin shared only 67% of hydrogen-bond interactions and 67% of non-hydrogen interactions with the native ligand. The compound sanguinine also formed identical hydrogen-bond and non-hydrogen interactions with the native ligand. Its binding energy was –8.3 kcal/mol, again surpassing the native ligand (–5.6 kcal/mol). However, it maintained only 67% of hydrogen-bond interactions and 67% of non-hydrogen interactions in common with the native ligand.

The compound stigmasterol exhibited both hydrogen-bond and non-hydrogen interactions consistent with the native ligand. Its binding energy was –8.3 kcal/mol, also superior to the native ligand (–5.6 kcal/mol). Yet, similar to sanguinine, it shared only 67% of hydrogen-bond interactions and 67% of non-hydrogen interactions with the native ligand. Taken together, the analysis of binding energy and amino acid interactions for the five compounds—24-hydroxyecdysone, ecdysone, quercetin, sanguinine, and stigmasterol—suggests that ecdysone exhibits the most promising binding profile with PBP2a. Ecdysone not only displayed the strongest binding energy compared to the native ligand and the other four test compounds but also maintained a higher degree of similarity in both hydrogen-bond and non-hydrogen interactions relative to the native ligand (Alexander et al., 2020).

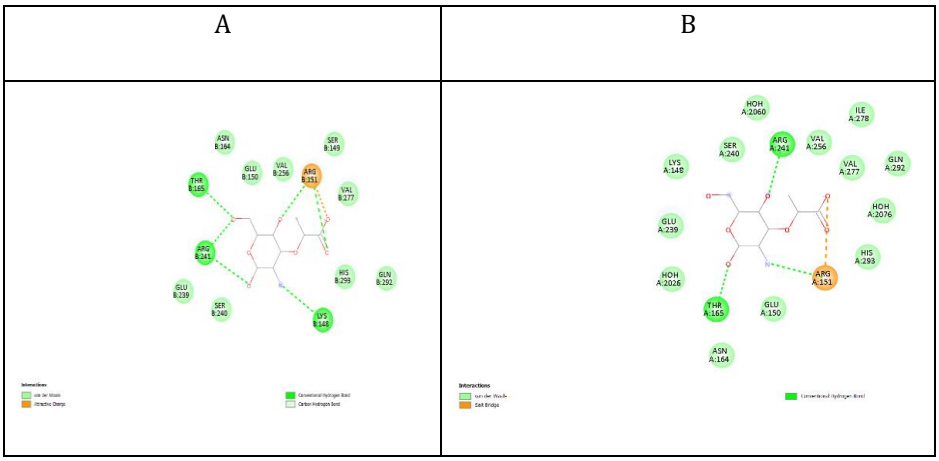

Figure 5. Interaksi Asam Amino Ligan Asli (A) dan Ecdysone (B) Pada Protein Target Pbp2a

The interaction analysis of the native ligand (a) and ecdysone (b) with the target protein PBP2a revealed that both shared identical hydrogen-bond interactions with residues THR:165 and ARG:241, as well as common non-hydrogen interactions with residues LYS:148, GLU:239, ASN:164, GLU:150, ARG:151, HIS:293, VAL:277, VAL:256, and SER:240. In addition, both the native ligand and ecdysone demonstrated van der Waals interactions with residues GLU:239, SER:240, HIS:293, GLN:292, VAL:277, VAL:256, GLU:150, and ASN:164 (Lee et al., 2018).

The protein PBP2a (Penicillin-Binding Protein 2a) is a key enzyme involved in the mechanism of β-lactam antibiotic resistance in *Staphylococcus aureus*, particularly in methicillin-resistant strains (MRSA). The survival of MRSA depends heavily on PBP2a, as this enzyme continues to catalyze peptidoglycan synthesis even in the presence of β-lactam antibiotics, which typically inhibit other PBPs. PBP2a possesses an active site with markedly reduced affinity for β-lactams, thereby maintaining cell wall biosynthesis and ensuring bacterial viability (Fuda et al., 2005). In this study, amino acid interaction analysis revealed that the antibacterial activity of PBP2a is not solely associated with ARG:241, but also involves several other critical residues such as LYS:316, ASN:146, and GLY:307. Both the native ligand (A) and ecdysone (B) were shown to interact with some of these key residues located near or within the catalytic site of PBP2a. While ARG:241 is frequently observed in ligand interactions, its contribution to antibacterial activity is not always dominant. By contrast, LYS:316 plays a direct role in the transpeptidation process, an essential step in bacterial cell wall synthesis. Interactions between ligands and this residue may therefore significantly impair the enzymatic function of PBP2a. The ability of ecdysone to establish interactions with these residues highlights its potential as a PBP2a inhibitor, as it may disrupt the protein's catalytic function and compromise the cell wall integrity of MRSA (Shamsi et al., 2021).

Molecular Dynamics Simulation Analysis

In this study, the best candidate compounds derived from *Sidaguri* were docked with their respective protein targets and subsequently evaluated using molecular dynamics (MD) simulations with YASARA Dynamics

SCCMec (4FAK)

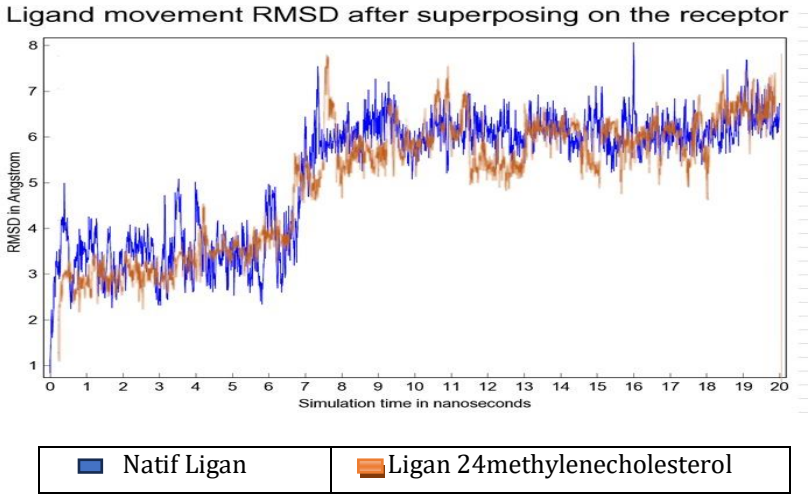

Figure 6. Grafik RMSD SCCMec

The parameters RMSD (Root Mean Square Deviation) and RMSF (Root Mean Square Fluctuation) were employed to evaluate the stability of the protein throughout the simulation. The RMSD values of both the ligand and protein were calculated from the trajectory plots, and the initial values were recorded at the beginning of the simulation, as shown in Figure 18. For the compound 24-methylenecholesterol bound to the target protein SCCMec, the simulation initially showed an increase in RMSD from 1.5 to 2.5 Å. After 0.2 ns, the RMSD further

MEDFARM: Jurnal Farmasi dan Kesehatan, Vol. 14, No. 2, 2025, Page 575-601
e-ISSN : 2715-9957
p-ISSN: 2354-8487

increased to a range of 2.5–3.2 Å. A slight decrease to 3 Å was observed at 0.5 ns, after which the RMSD stabilized between 8–20 ns, maintaining an average value of approximately 6 Å. In contrast, the native ligand of SCCMec exhibited an initial rise in RMSD from 1 to 5 Å at the onset of the simulation (0.00 ns). Stability was observed between 1–6.5 ns, with an average RMSD of 3 Å. A sharp increase to 7.2 Å occurred at 6.7–7 ns, followed by a decrease to 6 Å at 7–7.5 ns. Beyond this point, the RMSD values remained stable, averaging approximately 6 Å until the end of the simulation.

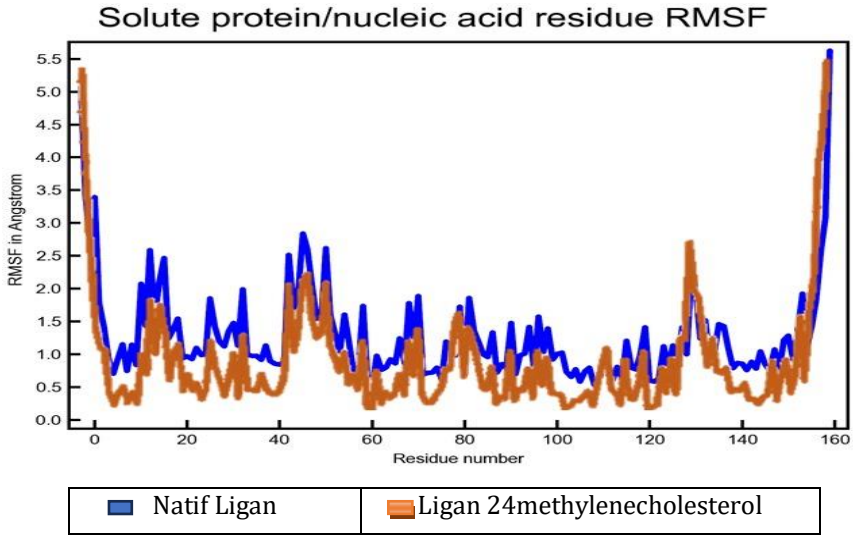

Figure 7. Grafik RMSF SCCMec

The RMSF values indicated low and stable fluctuations for most residues, remaining within the range of 0.5–1.5 Å throughout the simulation period, as shown in Figure 19. A notable increase in RMSF was observed at residue 40, reaching 2.0 Å. Such elevated fluctuations suggest that this residue is more flexible and susceptible to structural changes. Consequently, 24-methylenecholesterol was found to influence the dynamic behavior of the protein. At the end of the simulation, the RMSF values increased to 5.4 Å for the compound and 5.5 Å for the native ligand. For the majority of residues, however, fluctuations were comparable to those of the native ligand in the target protein SCCmec. The relatively low fluctuation values confirm the presence of a strong ligand–protein interaction. Furthermore, 24-methylenecholesterol shared the same hydrogen-bonding interactions with the native ligand, particularly with residues GLY108 and THR104, both exhibiting RMSF values below 2 Å, thereby indicating structural stability (Rashid et al., 2022).

FtsZ (8HTB)

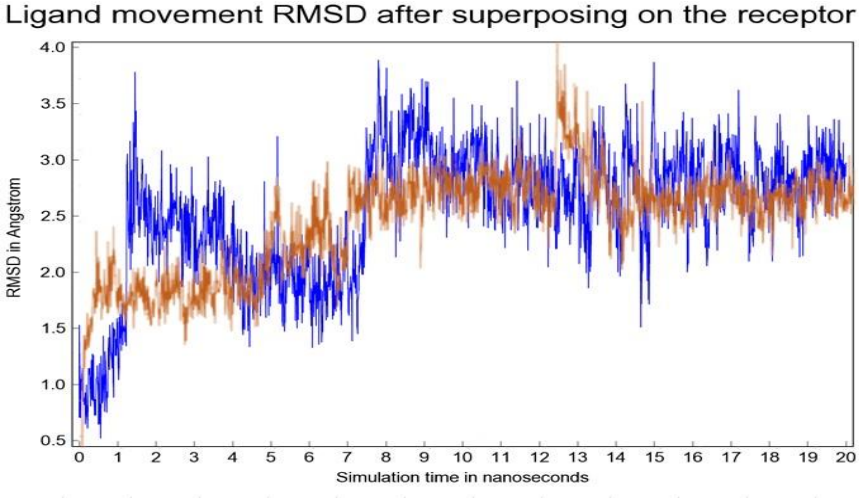

Figure 8. Grafik RMSD FtsZ

The parameters RMSD (Root Mean Square Deviation) and RMSF (Root Mean Square Fluctuation) were employed to evaluate the stability of the protein during the simulation. The RMSD values for both ligand and protein were derived from the simulation graphs, with the initial values recorded at the beginning of the trajectory, as shown in Figure 20. For the quercetin–FtsZ protein complex, the RMSD increased from 0.5 to 1.3 Å at the start of the simulation. After 1.0 ns, the RMSD further rose from 1.3 to 2.3 Å. A slight decrease was observed at 1.5 ns, where the RMSD stabilized at approximately 2.0 Å. From 8 to 20 ns, the complex exhibited consistent stability, maintaining an average RMSD of 2.5 Å. For the native ligand–FtsZ complex, the RMSD increased from 0.7 to 1.5 Å at the beginning of the simulation (0.00 ns). Stability was observed during the intervals 4–7 ns and 8–20 ns, with an average RMSD value of 2.7 Å.

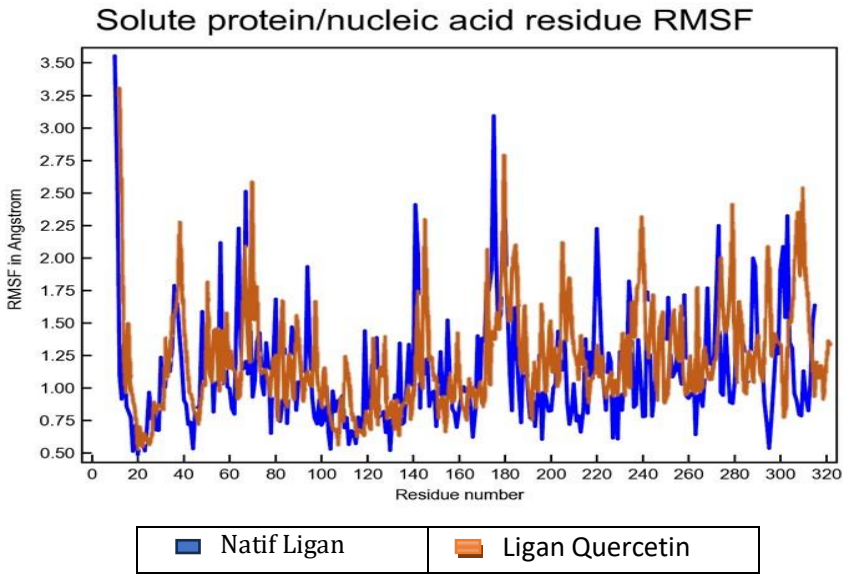

Figure 9. RMSF Graph of FtsZ

The RMSF (Root Mean Square Fluctuation) values indicate low and stable fluctuations for most residues, remaining within the range of 0.75–1.50 Å throughout the simulation period, as shown in Figure 21. An increase in RMSF values was observed around residue 180, reaching up to 2.75 Å. Such elevated fluctuations suggest that this residue is more flexible and susceptible to structural changes, implying that the compound quercetin influences the dynamic behavior of the protein. At the end of the simulation, the RMSF value for quercetin increased to 1.25 Å, while that of the native ligand rose to 1.50 Å. For the majority of residues, fluctuations were comparable to those of the native ligand bound to the target protein FtsZ. The overall low fluctuation values confirm the formation of a stable and strong ligand–protein interaction. Furthermore, quercetin exhibited hydrogen bond interactions with the same amino acids as the native ligand, namely GLY108,

PHE132, and LEU76, all maintaining fluctuations below 2 Å, thereby indicating structural stability (Rashid et al., 2022).

Conclusion

Based on the findings of this study, it can be concluded that ten compounds derived from *Sidaguri*—namely acacetin, ecdysone, peganine, kaempferol, sanguinine, quercetin, 24-methylenecholesterol, quindolinone, stigmasterol, and campesterol—were predicted to exhibit strong binding affinity toward MRSA target proteins. Among these, ecdysone showed favorable interaction models and high binding affinity with the target proteins 4CJN and 6O9S, quercetin demonstrated strong interactions and affinity with 8HTB, and 24-methylenecholesterol displayed favorable interactions and binding affinity with 4FAK. Furthermore, quercetin, ecdysone, and 24-methylenecholesterol exhibited stable protein–ligand interactions throughout molecular simulations, suggesting their potential as effective inhibitors. In addition, fifteen *Sidaguri*-derived compounds, including 2D-hydroxyecdysone, acacetin, ecdysone, peganine, vasicinol, vasicinone, kaempferol, pterosterone, sanguinine, quercetin, 24-methylenecholesterol, scopoletin, quindolinone, stigmasterol, and campesterol, were predicted to possess favorable pharmacokinetic profiles, thus reinforcing their promise as potential drug candidates against MRSA infections.

Declaration of Competing Interest

The author declare no competing interests related to this research. There are no financial, personal, or professional conflicts that could affect the research outcomes

Reference

Adnan, S. N. A., Ibrahim, N., & Yaacob, W. A. (2017). Transcriptome analysis of methicillin-resistant Staphylococcus aureus in response to stigmasterol and lupeol. *Journal of Global Antimicrobial Resistance*, *8*, 48–54. https://doi.org/10.1016/j.jgar.2016.10.006

Ali, M., Muhammad, S., Gul, M., & Khan, A. (2019). Antimicrobial and bronchodilator potential of alkaloids from Adhatoda vasica. *Biomedicine & Pharmacotherapy*, 111, 10401046. https://doi.org/10.1016/j.biopha.2018.12.140

Asri, R. C., Rasyid, R., & Edison, E. (2017). Identifikasi MRSA pada Diafragma Stetoskop di Ruang Rawat Inap dan HCU Bagian Penyakit Dalam. *Jurnal Kesehatan Andalas*, *6*(2), 239. https://doi.org/10.25077/jka.v6i2.685

Bakal, R. L., Jawarkar, R. D., Manwar, J. V., Jaiswal, M. S., Ghosh, A., Gandhi, A., Zaki, M. E. A., Al-Hussain, S., Samad, A., Masand, V. H., Mukerjee, N., Nasir Abbas Bukhari, S., Sharma, P., & Lewaa, I. (2022). Identification of potent aldose reductase inhibitors as antidiabetic (Anti-hyperglycemic) agents using QSAR based virtual Screening, molecular Docking, MD simulation and MMGBSA approaches: Identification of potent aldose reductase inhibitors as antidiabet. *Saudi Pharmaceutical Journal*, *30*(6), 693–710. https://doi.org/10.1016/j.jsps.2022.04.003

Beuria, T. K., Mullapudi, S., Mileykovskaya, E., Sadasivam, M., & Margolin, W. (2005).

Adenine nucleotide-dependent regulation of FtsZ polymer dynamics by Mycobacterium tuberculosis FtsZ-binding protein. *Journal of Biological Chemistry*, 280(43), 40852–40860.

Boundy, S., Safo, M. K., Wang, L., Musayev, F. N., O'Farrell, H. C., Rife, J. P., & Archer, G. L. (2013). Characterization of the Staphylococcus aureus rRNA methyltransferase encoded by orfx, the gene containing the staphylococcal chromosome cassette mec (SCCmec) insertion site. *Journal of Biological Chemistry*, *288*(1), 132–140. https://doi.org/10.1074/jbc.M112.385138

Burley, S. K., Bhikadiya, C., Bi, C., Bittrich, S., Chen, L., Crichlow, G. V, Christie, C. H., Dalenberg, K., Costanzo, L. Di, Duarte, J. M., Dutta, S., Feng, Z., Ganesan, S., Goodsell, D. S., Ghosh, S., Green, R. K., Guzenko, D., Hudson, B. P., Lawson, C. L., … Zhuravleva, M. (2021). *RCSB Protein Data Bank : powerful new tools for exploring 3D structures of biological macromolecules for basic and applied research and education in fundamental biology , biomedicine , biotechnology , bioengineering and energy sciences*. *49*(November 2020), 437–451. https://doi.org/10.1093/nar/gkaa1038

Cong, Y., Yang, S., & Rao, X. (2020). Vancomycin resistant Staphylococcus aureus infections: A review of case updating and clinical features. *Journal of Advanced Research*, *21*, 169–176. https://doi.org/10.1016/j.jare.2019.10.005

Daina, A., Michielin, O., & Zoete, V. (2017). SwissADME: A free web tool to evaluate pharmacokinetics, drug-likeness and medicinal chemistry friendliness of small molecules. *Scientific Reports*, *7*(March), 1.13. https://doi.org/10.1038/srep42717

den Blaauwen, T., Hamoen, L. W., & Levin, P. A. (2017). The divisome at 25: the road ahead. *Current Opinion in Microbiology*, *36*, 85,94. https://doi.org/10.1016/j.mib.2017.01.007

Dewi, R. S., Anggraeni, A., Bahti, H. H., Yusuf, M., Hardianto, A., & Mutholib, A. (2022). Simulasi Dinamika Molekuler Ligan Disekunderbutil ditiofosfat (DSBDTP) Untuk Ekstraksi Logam Tanah Jarang. *SainsMath: Jurnal MIPA Sains Terapan*, *20*(3), 1–9.

Dwi Agistia, D., Purnomo, H., Tegar, M., & Endro Nugroho, A. (2013). Interaction Between Active Compounds From Aegle marmelos Correa As Anti Inflammation Agent With Cox-1 And Cox-2 Receptor Interaksi Senyawa Aktif Dari Aegle marmelos Correa Sebagai Anti Inflamasi Dengan Reseptor Cox-1 Dan Cox-2. *Traditional Medicine Journal*, *18*(2), 2013.

Huey, R. B., Kearney, M. R., Krockenberger, A., Holtum, J. A. M., Jess, M., & Williams, S. E. (2012). Predicting organismal vulnerability to climate warming: Roles of behaviour, physiology and adaptation. *Philosophical Transactions of the Royal Society B: Biological Sciences*, *367*(1596), 1665–1679. https://doi.org/10.1098/rstb.2012.0005

Jing, S., Kong, X., Wang, L., Wang, H., Feng, J., Wei, L., Meng, Y., Liu, C., Chang, X., Qu, Y., Guan, J., Yang, H., Zhang, C., Zhao, Y., & Song, W. (2022). Quercetin Reduces the Virulence of S. aureus by Targeting ClpP to Protect Mice from MRSA-Induced Lethal Pneumonia. *Microbiology Spectrum*, *10*(2). https://doi.org/10.1128/spectrum.02340-21

Land, H., & Humble, M. S. (2018). YASARA : A Tool to Obtain Structural Guidance in Biocatalytic Investigations. In *Protein Enginering : Methods and Protocol* (Vol. 1685, pp. 43–67). https://doi.org/10.1007/978-1-4939-7366-8

Llarrull, L. I., Fisher, J. F., & Mobashery, S. (2009). Molecular basis and phenotype of methicillin resistance in Staphylococcus aureus and insights into new β-lactams that meet the challenge. *Antimicrobial Agents and Chemotherapy*, *53*(10), 4051–4063. https://doi.org/10.1128/AAC.00084-09

Morris, G. M., Ruth, H., Lindstrom, W., Sanner, M. F., Belew, R. K., Goodsell, D. S., & Olson, A. J. (2009). Software news and updates AutoDock4 and AutoDockTools4: Automated docking with selective receptor flexibility. *Journal of Computational Chemistry*, *30*(16), 2785–2791. https://doi.org/10.1002/jcc.21256

Mukherjee, A. K., Ratha, S., Dhar, S., Debata, A. K., Acharya, P. K., Mandal, S., Panda, P. C., & Mahapatra, A. K. (2010). Genetic relationships among 22 Taxa of bamboo revealed by ISSR and EST-based random primers. *Biochemical Genetics*, *48*(11–12), 1015–1025. https://doi.org/10.1007/s10528-010-9390-8

Nandhini, P., Kumar, P., Mickymaray, S., Alothaim, A. S., Somasundaram, J., & Rajan, M. (2022). Recent Developments in Methicillin-Resistant Staphylococcus aureus (MRSA) Treatment: A Review. *Antibiotics*, *11*(5), 1–21. https://doi.org/10.3390/antibiotics11050606

Nes, W. D., Janssen, G. G., & Zhou, W. (2008). Biosynthesis and function of sterols. *International Journal of Plant Genomics*, 2008, Article ID 394623. https://doi.org/10.1155/2008/394623

Purnomo, H. (2019). *Moleculer Docking Parasetamol dan Analognya menggunakan PLANTS (Protein-Ligand ANT-System)* (D. Prabantini (ed.)). Rapha Publishing.

Sari, W. K., Advitasari, Y. D., & Elisa, N. (2024). Pola peresepan antibiotic untuk pengobatan infeksi saluran pernafasan atas (ISPA) di Klinik X Kota Semarang. *Cendekia Journal of Pharmacy*, *8*(1), 17–27.

Tegar, M., & Purnomo, H. (2013). Tea Leaves Extracted as Anti-Malaria based on Molecular Docking PLANTS. *Procedia Environmental Sciences*, *17*, 188–194. https://doi.org/10.1016/j.proenv.2013.02.028

Woldeyes, S., Adane, L., Tariku, Y., Muleta, D., & Begashaw, T. (2012). Natural Products Chemistry & Research Evaluation of Antibacterial Activities of Compounds Isolated From Sida rhombifolia linn.(Malvaceae). *Natural Products Chemistry & Research*, *1*(1), 1–8.

Zhang, T., Yang, X., Sun, M., & Wang, C. (2017). Crystal structures and antioxidant activity of acacetin and its derivatives. *Journal of Molecular Structure*, 1149, 386–392. https://doi.org/10.1016/j.molstruc.2017.08.027